Electronic supplementary information (ESI)

Extending the Family of Quinolone Antibacterials to New Copper Derivatives: Self-assembly, Structural and Topological Features, Catalytic and Biological Activity†

Panagiotis Xerras,[a] Anna-Maria Bacharidou,[b] Stavros Kalogiannis,[b] Franc Perdih,[c] Marina V. Kirillova,[d] Alexander M. Kirillov,[d,e,*] IztokTurel,[c,*] and George Psomas [a,*]

[a]*Department of General and Inorganic Chemistry, Faculty of Chemistry, Aristotle University of Thessaloniki, GR-54124 Thessaloniki, Greece. E-mail: gepsomas@chem.auth.gr*

[b]*Department of Nutrition and Dietetics, Faculty of Agriculture, Food Technology and Nutrition, Alexander Technological Educational Institution, Sindos, Thessaloniki, Greece.*

[c]*Faculty of Chemistry and Chemical Technology, University of Ljubljana, Vecna pot 113, 1000 Ljubljana, Slovenia. E-mail: Iztok.Turel@fkkt.uni-lj.si*

[d]*Centro de Química Estrutural, Instituto Superior Técnico, Universidade de Lisboa, Av. Rovisco Pais, 1049-001, Lisbon, Portugal. E-mail: kirillov@tecnico.ulisboa.pt*

[e]*Peoples' Friendship University of Russia (RUDN University), 6 Miklukho-Maklay st., Moscow, 117198, Russian Federation.*

*†Electronic supplementary information (ESI) contains: experimental protocols for biological studies; tables with crystallographic data and selected bonding parameters; the albumin constants; comparison of the biological activity; additional figures containing fluorescence emission UV-vis spectra and other data; crystallographic CIF files for **2**−**4** (CCDC 1844910–1844912). For ESI and crystallographic data in CIF or other electronic format see DOI: 10.1039/x0xx00000x*

Experimental Protocols

S1. Determination of Minimum Inhibitory Concentration

The antimicrobial activity of Hpef and complexes **1-4** was evaluated by determining the MIC values towards two Gram-(-) (*E. coli* and *X. campestris*) and two Gram-(+) (*S. aureus* and *B. subtilis*) bacterial species. Cultures of these microbial strains were grown on a rich selective agar medium and stored at 4°C. The selective media used were Nutrient Agar or Broth for *B. subtilis* and *S. aureus*, Yeast Mold Agar or Broth for *X. campestris* and Luria Agar or Broth for *E. coli*. Cells picked from the surface of the stored cultures were used to initiate liquid pre-cultures of the same selective medium at an initial turbidity of roughly 1 McFarland unit. Pre-cultures were incubated for 24 h in a rotary shaking incubator and subsequently they were used to inoculate the test cultures used for the determination of MIC at an initial turbidity of 0.5 McFarland units. The test cultures consisted of Mueller-Hinton broth (Deben Diagnostics Ltd) containing different concentrations of the compounds. Different concentrations were achieved as follows: the compounds were freshly dissolved in DMSO to a concentration of 1 mg/mL and they were diluted with DMSO, using the method of progressive double dilution. Thus, working solutions with decreasing concentrations of the compounds under investigation were achieved. The working solutions were subsequently diluted to the final desired concentration by addition to the growth medium at a proportion of 2:98. MIC values were determined as the lowest concentrations of the tested compounds that inhibited visible growth of each respective organism after a 24 h incubation.[1] Bacterial growth was determined by measuring the turbidity of appropriately diluted cultures at 600 nm with reference to equally diluted sterile growth medium and the inhibition achieved was calculated by comparing the turbidity of each culture to the average of the turbidity of three non-inhibited cultures. All test cultures were grown in triplicates and for the determination of MIC, growth had to be inhibited in at least two cultures of the triplicate. Incubation temperature at all stages was 37°C except for *X. campestris* that was cultivated at 28°C.

S2. Interaction with Serum Albumins

The albumin binding studies were performed by tryptophan fluorescence quenching experiments using BSA (3 μM) or HSA (3 μM) in buffer (containing 15 mM trisodium citrate and 150 mM NaCl at pH 7.0). The quenching of the emission intensity of tryptophan residues of BSA at 343 nm or HSA at 351 nm was monitored using Hpef or its Cu(II) complexes **1**-**4** as quenchers with increasing concentration.[2] Fluorescence spectra were recorded in the range 300-500 nm with an excitation wavelength of 295 nm. The fluorescence emission spectra of the free compounds were also recorded under the same experimental conditions, i.e. excitation at 295 nm, and a maximum

emission band appeared at 410 nm. Therefore, the quantitative studies of the SA fluorescence emission spectra were performed after their correction by subtracting the spectra of the complexes.

The extent of the inner-filter effect can be roughly estimated with the following formula:

$$I_{corr} = I_{meas} \times 10^{\frac{\varepsilon(\lambda_{exc})cd}{2}} \times 10^{\frac{\varepsilon(\lambda_{em})cd}{2}} \qquad \text{(eq. S1)}$$

where I_{corr} = corrected intensity, I_{meas} = the measured intensity, c = the concentration of the quencher, d = the cuvette (1 cm), $\varepsilon(\lambda_{exc})$ and $\varepsilon(\lambda_{em})$ = the ε of the quencher at the excitation and the emission wavelength, respectively, as calculated from the UV-vis spectra of the complexes.[3]

The Stern-Volmer and Scatchard graphs are used in order to study the interaction of a quencher with serum albumins. According to Stern-Volmer quenching equation:[4]

$$\frac{Io}{I} = 1 + k_q \tau_0 [Q] = 1 + K_{SV}[Q] \qquad \text{(eq. S2)}$$

where Io = the initial tryptophan fluorescence intensity of SA, I = the tryptophan fluorescence intensity of SA after the addition of the quencher (i.e. Hpef and its complexes **1-4**), k_q = the quenching constant, K_{SV} = the Stern-Volmer constant, τ_o = the average lifetime of SA without the quencher, [Q] = the concentration of the quencher) K_{SV} (M^{-1}) can be obtained by the slope of the diagram Io/I versus [Q], and subsequently the quenching constant (k_q, $M^{-1}s^{-1}$) is calculated from eq. S3, with $\tau_o = 10^{-8}$ s as fluorescence lifetime of tryptophan in SA,

$$K_{SV} = k_q \tau_o \qquad \text{(eq. S3)}$$

From the Scatchard equation:

$$\frac{\Delta I / Io}{[Q]} = nK - K\frac{\Delta I}{Io} \qquad \text{(eq. S4)}$$

where n is the number of binding sites per albumin and K is the SA-binding constant, K (in M^{-1}) is calculated from the slope in plots (ΔI/Io)/[Q] *versus* ΔI/Io and n is given by the ratio of y intercept to the slope.[4]

S3. Interaction with CT DNA Studied by UV-vis Spectroscopy

The interaction of Hpef and complexes **1-4** with CT DNA was studied by UV-vis spectroscopy in order to examine the possible binding mode to CT DNA and to determine the corresponding DNA-binding constants (K_b). The UV-vis spectra of a CT DNA solution (0.15-0.18 mM) were recorded in the presence of each compound at diverse [compound]/[DNA] ratios (= *r*). Control experiments with DMSO were performed and no changes in the spectra of CT DNA were observed.

The K_b constants (in M^{-1}) were determined using the UV-vis spectra of the compounds recorded for a constant concentration (10-20 μM) in the presence of DNA for increasing *r* values.

The value of K_b is given by the ratio of slope to the y intercept in plots [DNA]/(ε_A-ε_f) *versus* [DNA], according to the Wolfe-Shimer equation (eq. S5):[5]

$$\frac{[DNA]}{(\varepsilon_A - \varepsilon_f)} = \frac{[DNA]}{(\varepsilon_b - \varepsilon_f)} + \frac{1}{K_b(\varepsilon_b - \varepsilon_f)} \qquad \text{(eq. S5)}$$

where [DNA] is the concentration of DNA in base pairs, $\varepsilon_A = A_{obsd}/[compound]$, ε_f = the extinction coefficient for the free compound and ε_b = the extinction coefficient for the compound in the fully bound form.

S4. Interaction with CT DNA Studied by Viscometry

The DNA-binding mode of the compounds may be clarified by monitoring the DNA-viscosity changes in the presence of the compounds, since the DNA-viscosity changes (η/η_0) are dependent on the relative DNA-length changes (L/L_0) in the presence of a DNA-binder and are related by the equation $L/L_0 = (\eta/\eta_0)^{1/3}$. When this binding takes place *via* classic intercalation, the DNA-base pairs will be separated providing enough space for the intercalating compound; as a result the relative DNA-length will increase followed by an increase in DNA viscosity. When the compound binds in DNA-grooves by partial and/or non-classic intercalation, a bend or kink in the DNA helix may occur resulting in a slight reduce of the effective DNA-length; in this case, the DNA-viscosity is slightly decreased or remains unchanged.[6] The viscosity of DNA ([DNA] = 0.1 mM) in buffer solution (150 mM NaCl and 15 mM trisodium citrate at pH 7.0) was measured in the presence of increasing amounts of Hpef and its complexes (up to the value of r = 0.36). All measurements were performed at room temperature. The obtained data are presented as $(\eta/\eta_0)^{1/3}$ *versus r*, where η is the viscosity of DNA in the presence of the compound, and η_0 is the viscosity of DNA alone in buffer solution.

S5. Displacement of EB Studied by Fluorescence Emission Spectroscopy

The competitive studies of each compound with EB were investigated by fluorescence emission spectroscopy in order to investigate if the complexes can displace EB from its DNA-EB complex. The DNA-EB conjugate was prepared by adding 20 μM EB and 26 μM CT DNA in buffer (150 mM NaCl and 15 mM trisodium citrate at pH 7.0). The possible intercalating effect of the complexes was studied by adding a certain amount of a solution of the compound step by step into a solution of the pre-treated EB-DNA conjugate. The influence of the addition of each complex to the DNA-EB complex solution was obtained by recording the changes of fluorescence emission spectra with excitation wavelength at 540 nm. Hpef and its complexes **1-4** show no fluorescence at room temperature in solution or in the presence of DNA under the same experimental conditions;

therefore, the observed quenching is attributed to the displacement of EB from its EB-DNA complex.

The Stern-Volmer constant (K_{SV}, in M^{-1}) has been used to evaluate the quenching efficiency and the K_{sv} values have been calculated according to the linear Stern-Volmer equation (eq. S2),[7] where Io and I are the emission intensities of the EB-DNA solution in the absence and the presence of the quencher (i.e. Hpef and its complexes **1-4**), respectively, [Q] is the concentration of the quencher, τ_o = the average lifetime of the emitting system without the quencher and k_q = the quenching constant. K_{SV} was obtained from the Stern-Volmer plots by the slope of the plots Io/I *versus* [Q]. Taking τ_o = 23 ns as the fluorescence lifetime of the EB-DNA system,[8] the quenching constants (k_q, $M^{-1}s^{-1}$) of the complexes were calculated according to eq. S3.

References

1 J.M. Andrews, *J. Antimicr. Chemotherapy*, 2001, **48(S1)**, 5-16.

2 J.R. Lakowicz, *Principles of Fluorescence Spectroscopy*, third ed.; Springer: New York, 2006.

3 L. Stella, A.L. Capodilupo and M. Bietti, *Chem. Commun*., 2008, 4744-4746

4 Y. Wang, H. Zhang, G. Zhang, W. Tao and S. Tang, *J. Luminescence,* 2007, **126**, 211-218.

5 A. Wolfe, G. Shimer and T. Meehan, *Biochemistry,* 1987, **26**, 6392-6396.

6 J.L. Garcia-Gimenez, M. Gonzalez-Alvarez, M. Liu-Gonzalez, B. Macias, J. Borras and G. Alzuet, *J. Inorg. Biochem.,* 2009, **103**, 923-934.

7 G. Zhao, H. Lin, S. Zhu, H. Sun and Y. Chen, *J. Inorg. Biochem*., 1998, **70**, 219-226.

8 D.P. Heller and C.L. Greenstock, *Biophys. Chem*., 1994, **50**, 305-312.

Tables

Table S1. Crystallographic data for complexes **2**·2H_2O, **3**·MeOH·2H_2O and **4**·0.5MeOH·4H_2O.

	2·2H_2O	**3**·MeOH·2H_2O	**4**·0.5MeOH·4H_2O
Empirical formula	$C_{27}H_{32}ClCuFN_6O_5$	$C_{30}H_{35}ClCuFN_5O_6$	$C_{55}H_{74}C_{l2}Cu_2F_2N_{10}O_{15}$
M_w	638.58	679.62	1351.22
T, K	293(2)	150(2)	293(2)
Crystal system	Triclinic	Monoclinic	Monoclinic
Space group	P -1	P 21/n	P 21/c
a (Å)	8.0898(3)	10.8217(2)	17.0082(2)
b (Å)	11.8193(4)	24.4873(7)	24.7830(5)
c (Å)	15.4407(5)	11.4809(2)	14.5284(3)
α (°)	99.797(3)	90.00	90.00
β (°)	91.722(2)	98.870(2)	97.631(2)
γ (°)	92.749(3)	90.00	90.00
V (Å^3)	1452.07(9)	3005.99(11)	6069.69(19)
Z	2	4	4
D_{calc} (g/cm^3)	1.461	1.502	1.479
μ (mm^{-1})	0.898	0.874	0.869
Data collected / unique / [I>2σ(I)]	14012 / 6654 / 5217	16879 / 6872 / 5514	33231 / 13894/ 10660
Restraints / parameters	5 / 387	0 / 407	16 / 823
F(000)	662	1412	2816
GOF on F^2	1.050	1.039	1.033
R_1 / wR_2 (all data)	0.0552/0.1070	0.0619/0.1303	0.0680/0.1386
R_1 / wR_2[I>2σ(I)]	0.0393/0.0978	0.0470/0.1185	0.0485/0.1255

Table S2. Selected bond distances (Å), bond angles (º) and structural parameters (T^5, τ) for complexes **2**-**4**.

	2	**3**	**4**
Bond distances (Å)			
Cu(1)-O(1)	1.9200(17)	1.912(2)	1.919(2)
Cu(1)-O(3)	1.9548(15)	1.946(2)	1.9525(19)
Cu(1)-N(1)	2.0156(19)	2.023(2)	2.005(2)
Cu(1)-N(2)	2.015(2)	2.022(2)	2.017(2)
Cu(1)-Cl(1)	2.5608(7)	2.5124(7)	2.5415(8)
O(1)-C(1)	1.282(3)	1.285(3)	1.278(3)
C(1)-O(2)	1.230(2)	1.234(4)	1.233(3)
O(3)-C(4)	1.279(2)	1.287(3)	1.281(3)
Bond angles (°)			
O(1)-Cu(1)-O(3)	90.15(7)	92.47(9)	92.46(8)
O(1)-Cu(1)-N(1)	166.03(8)	163.44(9)	162.65(9)
O(1)-Cu(1)-N(2)	88.90(8)	89.22(9)	89.68(10)
O(1)-Cu(1)-Cl(1)	101.85(6)	100.68(7)	98.02(7)
O(3)-Cu(1)-N(1)	89.67(7)	93.18(9)	93.35(9)
O(3)-Cu(1)-N(2)	170.08(8)	165.57(9)	165.10(9)
O(3)-Cu(1)-Cl(1)	94.60(5)	92.87(6)	90.86(6)
N(1)-Cu(1)-N(2)	88.88(8)	81.53(9)	80.66(10)
N(1)-Cu(1)-Cl(1)	92.09(6)	94.56(6)	98.22(7)
N(2)-Cu(1)-Cl(1)	95.26(7)	100.90(7)	103.45(7)
Tetragonality, T^5	0.772	0.786	0.776
Trigonality index, τ	0.068	0.036	0.041

Table S3. The BSA and HSA binding constants and parameters (K_{sv}, k_q, K, n) for Hpef and its Cu(II) complexes **1-4**.

Compound	**Ksv (M^{-1})**	**k_q (M^{-1} s^{-1})**	**K (M^{-1})**	**n**
BSA				
pefloxacin	$8.46(\pm0.10)\times10^{3}$	$8.46(\pm0.10)\times10^{11}$	$2.51(\pm0.12)\times10^{5}$	0.21
[Cu(pef)$_2$(MeOH)], **1**	$1.69(\pm0.05)\times10^{5}$	$1.69(\pm0.05)\times10^{13}$	$1.77(\pm0.06)\times10^{5}$	1.00
[Cu(pef)(bipyam)Cl], **2**	$1.26(\pm0.07)\times10^{5}$	$1.26(\pm0.07)\times10^{13}$	$8.65(\pm0.37)\times10^{5}$	0.80
[Cu(pef)(phen)Cl], **3**	$1.04(\pm0.05)\times10^{5}$	$1.04(\pm0.05)\times10^{13}$	$9.50(\pm0.10)\times10^{4}$	1.04
[Cu(pef)(bipy)Cl], **4**	$5.52(\pm0.26)\times10^{4}$	$5.52(\pm0.26)\times10^{12}$	$1.14(\pm0.08)\times10^{5}$	0.76
HSA				
pefloxacin	$1.15(\pm0.12)\times10^{4}$	$1.15(\pm0.12)\times10^{12}$	$5.13(\pm0.35)\times10^{5}$	0.19
[Cu(pef)$_2$(MeOH)], **1**	$2.64(\pm0.15)\times10^{4}$	$2.64(\pm0.15)\times10^{12}$	$1.56(\pm0.43)\times10^{4}$	1.41
[Cu(pef)(bipyam)Cl], **2**	$6.05(\pm0.40)\times10^{4}$	$6.05(\pm0.40)\times10^{12}$	$1.23(\pm0.10)\times10^{5}$	0.75
[Cu(pef)(phen)Cl], **3**	$5.46(\pm0.25)\times10^{4}$	$5.46(\pm0.25)\times10^{12}$	$1.24(\pm0.06)\times10^{5}$	0.60
[Cu(pef)(bipy)Cl], 4	$1.53(\pm0.11)\times10^{4}$	$1.53(\pm0.11)\times10^{12}$	$4.78(\pm0.40)\times10^{4}$	0.46

Table S4. Minimum inhibitory concentration (MIC, in $\mu g \cdot mL^{-1}$) of diverse copper(II)-quinolone complexes against the microorganisms tested.

Compound	*EC* [a]	*SA* [a]	*PA* [a]	*BS* [a]	*XS* [a]	**Ref** [c]
Hflmq (Flumequine) (1st generation)	1	16	NT	2	8	1
Hoxo (Oxolinic acid) (1st generation)	1	16	16	NT [b]	NT	2
HPPA (pipemidic acid) (1st generation)	64.0	16.0	64.0	NT	NT	3
Herx (enrofloxacin) (2nd generation)	1.0	8.0	1.0	NT	NT	4
Hpef (pefloxacin) (2nd generation)	0.5	0.25	NT	0.5	0.5	5
Hpr-norf (N-propyl-norfloxacin) (2nd generation)	4.0	16.0	4.0	NT	NT	3
Hgati (gatifloxacin) (3rd generation)	0.063	0.125	NT	0.125	0.25	6
Hsf (sparfloxacin) (3rd generation)	8	0.5	0.25	NT	NT	7
$[Cu(flmq)_2(H_2O)_2]$	2	>64	NT	2	8	1
[Cu(flmq)(bipyam)Cl]	2	32	NT	4	8	1
[Cu(flmq)(phen)Cl]	2	32	NT	2	8	1
[Cu(flmq)(bipy)Cl]	2	32	NT	4	8	1
$[Cu(oxo)_2(H_2O)]$	64	64	32	NT	NT	2
[Cu(oxo)(bipyam)Cl]	64	64	64	NT	NT	2
[Cu(oxo)(phen)Cl]	64	32	64	NT	NT	2
[Cu(oxo)(bipy)Cl]	64	64	32	NT	NT	2
$[Cu(PPA)_2(H_2O)]$	8	16	8	NT	NT	3
[Cu(PPA)(bipyam)Cl]	16	32	16	NT	NT	3
[Cu(PPA)(phen)Cl]	4	8	4	NT	NT	3
[Cu(PPA)(bipy)Cl]	8	8	16	NT	NT	3
$[Cu(erx)_2(H_2O)]$	0.125	4	0.125	NT	NT	4
[Cu(erx)(phen)Cl]	2	4	1	NT	NT	4
$[Cu(erx)(bipy)(H_2O)]Cl$	1	4	0.5	NT	NT	4
$[Cu(pef)_2(MeOH)]$, **1**	0.5	0.25	NT	1	0.5	5
[Cu(pef)(bipyam)Cl], **2**	1	0.5	NT	1	1	5
[Cu(pef)(phen)Cl], **3**	1	0.5	NT	1	1	5
[Cu(pef)(bipy)Cl], **4**	1	0.5	NT	2	1	5
$[Cu(pr\text{-}norf)_2(H_2O)]$	0.5	8	8	NT	NT	3
[Cu(pr-norf)(bipyam)Cl]	4	8	4	NT	NT	3
[Cu(pr-norf)(phen)Cl]	2	16	0.25	NT	NT	3
[Cu(pr-norf)(bipy)Cl]	0.25	8	8	NT	NT	3
$[Cu(gati)_2(H_2O)]$	0.25	0.5	NT	0.5	0.5	6
[Cu(gati)(bipyam)Cl]	0.125	0.125	NT	0.25	0.5	6
[Cu(gati)(phen)Cl]	0.125	0.25	NT	0.25	1	6
[Cu(MOM-gati)(bipy)Cl]	0.25	0.25	NT	0.25	0.25	6
$[Cu(sf)_2]$	2	1	0.25	NT	NT	7
[Cu(sf)(bipyam)Cl]	2	4	1	NT	NT	7
[Cu(sf)(phen)Cl]	2	2	0.5	NT	NT	7
[Cu(sf)(bipy)Cl]	2	2	0.5	NT	NT	7

[a] *EC = E. coli, SA = S. aureus, PA = P. Aeruginosa, BS = B. subtilis, XC = X. campestris*

[b] NT = not tested

[c] References

1 I. Tsitsa, A. Tarushi, P. Doukoume, F. Perdih, A. de Almeida, A. Papadopoulos, S. Kalogiannis, A. Casini, I. Turel and G. Psomas, *RSC Adv*., 2016, **6**, 19555.

2 G. Psomas, A. Tarushi, Y. Sanakis, E. K. Efthimiadou, C.P. Raptopoulou and N. Katsaros, *J. Inorg. Biochem*., 2006, **100**, 1764.

3 E.K. Efthimiadou, N. Katsaros, A. Karaliota and G. Psomas, *Inorg. Chim. Acta*, 2007, **360**, 4093.

4 E.K. Efthimiadou, Y. Sanakis, M. Katsarou, C.P. Raptopoulou, A. Karaliota, N. Katsaros and G. Psomas, *J. Inorg. Biochem*., 2006, **100**, 1378.

5 Present work.

6 A. Kostelidou, S. Kalogiannis, O.A. Begou, F. Perdih, I. Turel and G. Psomas, *Polyhedron*, 2016, **119**, 359.

7 E.K. Efthimiadou, M.E. Katsarou, A. Karaliota and G. Psomas, *J. Inorg. Biochem*., 2008, **102**, 910

Table S5. The DNA- (K_b), HSA- ($K_{(HSA)}$) and BSA-binding ($K_{(BSA)}$) constants of reported Cu(II)-quinolone complexes.

Compound	K_b (M^{-1})	$K_{(HSA)}$ (M^{-1})	$K_{(BSA)}$ (M^{-1})	Ref [a]
Hflmq (flumequine)	3.53×10^5	2.37×10^6	6.67×10^4	1
Hnorf (norfloxacin)	4.07×10^4	7.20×10^5	1.73×10^4	2
Hoflo (ofloxacin)	3.91×10^4	2.73×10^4	5.88×10^4	2
Hpef (pefloxacin)	$6.05(\pm0.12)\times10^4$	$5.13(\pm0.35)\times10^5$	$2.51(\pm0.12)\times10^5$	3
Hgati (gatifloxacin)	$4.08(\pm0.34)\times10^4$	$7.54(\pm0.42)\times10^4$	$1.17(\pm0.05)\times10^5$	4
$[Cu(flmq)_2(H_2O)]$	8.39×10^3	7.55×10^4	4.29×10^4	1
[Cu(flmq)(bipyam)Cl]	1.07×10^5	1.58×10^5	2.62×10^5	1
[Cu(flmq)(phen)Cl]	2.39×10^5	1.28×10^5	3.24×10^5	1
[Cu(flmq)(bipy)Cl]	1.79×10^5	1.26×10^5	1.14×10^5	1
[Cu(Hnorf)(phen)Cl]Cl	1.83×10^6	4.22×10^4	7.09×10^4	2
$[Cu(Hnorf)_2]Cl_2\cdot6H_2O$	4.08×10^4	8.84×10^4	6.16×10^4	2
$[Cu(Hnorf)_2Cl_2]\cdot2H_2O$	1.97×10^4	4.27×10^4	5.56×10^4	2
$[Cu(Hoflo)_2][(CuCl_2)_2]$	2.56×10^6	4.51×10^4	4.51×10^4	2
$[Cu(pef)_2(MeOH)]$, **1**	$4.99(\pm0.14)\times10^5$	$1.56(\pm0.43)\times10^4$	$1.77(\pm0.06)\times10^5$	3
[Cu(pef)(bipyam)Cl], **2**	$8.46(\pm0.05)\times10^6$	$1.23(\pm0.10)\times10^5$	$8.65(\pm0.37)\times10^5$	3
[Cu(pef)(phen)Cl], **3**	$7.83(\pm0.35)\times10^4$	$1.24(\pm0.06)\times10^5$	$9.50(\pm0.10)\times10^4$	3
[Cu(pef)(bipy)Cl], **4**	$6.86(\pm0.20)\times10^5$	$4.78(\pm0.40)\times10^4$	$1.14(\pm0.08)\times10^5$	3
$[Cu(gati)_2(H_2O)]$	$4.81(\pm0.32)\times10^4$	$6.48(\pm0.26)\times10^4$	$2.96(\pm0.22)\times10^5$	4
[Cu(gati)(bipyam)Cl]	$2.10(\pm0.16)\times10^6$	$9.00(\pm0.26)\times10^4$	$1.27(\pm0.08)\times10^5$	4
[Cu(gati)(phen)Cl]	$5.24(\pm0.38)\times10^5$	$8.02(\pm0.34)\times10^4$	$1.36(\pm0.08)\times10^5$	4
[Cu(MOM-gati)(bipy)Cl]	$5.91(\pm0.10)\times10^5$	$8.63(\pm0.41)\times10^4$	$1.13(\pm0.06)\times10^5$	4

[a] References

1 E. Chalkidou, F. Perdih, I. Turel, D.P. Kessissoglou and G. Psomas, *J. Inorg. Biochem*., 2012, **113**, 55.

2 P. Zivec, F. Perdih, I. Turel, G. Giester and G. Psomas, *J. Inorg. Biochem*., 2012, **117**, 35.

3 Present work.

4 A. Kostelidou, S. Kalogiannis, O.A. Begou, F. Perdih, I. Turel and G. Psomas, *Polyhedron*, 2016, **119**, 359.

Figures

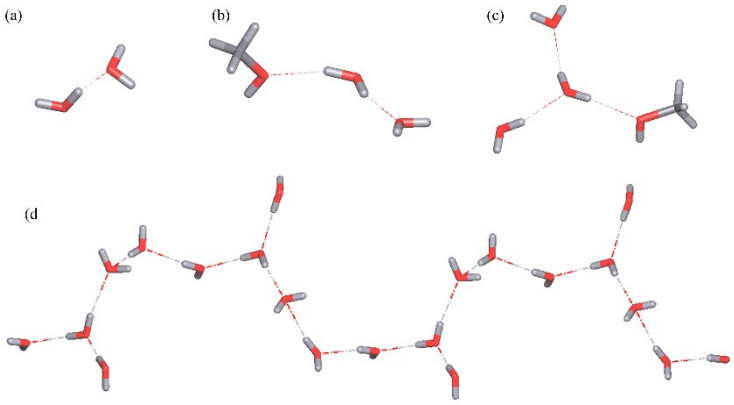

Figure S1. Different water or water-methanol associates identified in the crystal structures: (a) $(H_2O)_2$ dimer, (b) $(H_2O)_2(MeOH)$ trimer, (c) $(H_2O)_3(MeOH)$ tetramer, (d) infinite 1D $(H_2O)_{5n}$ tapes.

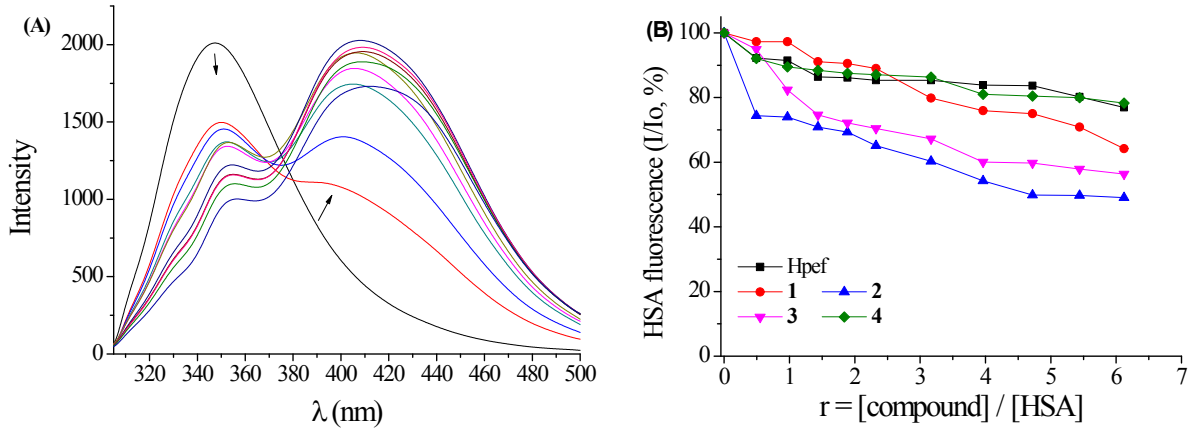

Figure S2. (A) Fluorescence emission spectra (λ_{exit} = 295 nm) for HSA ([HSA] = 3 μM) in buffer solution in the absence and presence of increasing amounts of **1** (r = [**1**]/[HSA] = 0-6.2). The arrows show the changes of intensity upon increasing amounts of the complexes. (B) Plot of relative HSA fluorescence intensity at λ_{em} = 351 nm (I/Io, %) *versus* r (r = [compound]/[HSA]) for Hpef and its complexes **1-4** (up to 77.0% of the initial HSA fluorescence for Hpef, 64.1 % for **1**, 49.0% for **2**, 56.3% for **3** and 78.2% for **4**) in buffer solution (150 mM NaCl and 15 mM trisodium citrate at pH 7.0). The fluorescence emission spectra of HSA exhibited in the presence of the compounds a significant quenching of the SA fluorescence emission band at $\lambda_{em,max}$ = 351 nm with the simultaneously appearance of a second emission band at 409 nm.

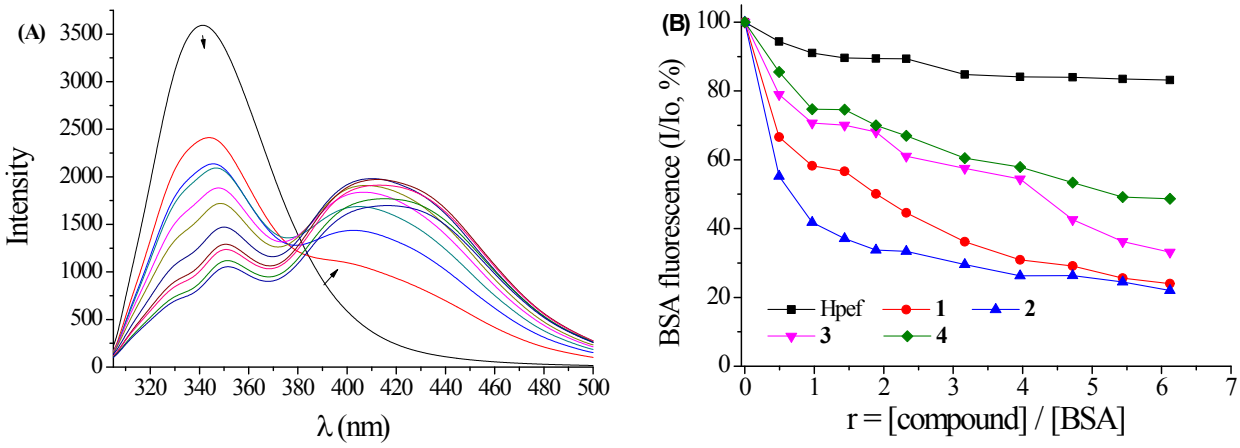

Figure S3. (A) Fluorescence emission spectra (λ_{exit} = 295 nm) for BSA ([BSA] = 3 μM) in buffer solution in the absence and presence of increasing amounts of **1** (r = [**1**]/[BSA] = 0-6.2). The arrows show the changes of intensity upon increasing amounts of the complexes. (B) Plot of relative BSA fluorescence intensity at λ_{em} = 343 nm (I/Io, %) *versus* r (r = [compound]/[BSA]) for Hpef and its complexes **1-4** (up to 83.2% of the initial BSA fluorescence for Hpef, 24.0 % for **1**, 22.0% for **2**, 33.1% for **3** and 48.7% for **4**) in buffer solution (150 mM NaCl and 15 mM trisodium citrate at pH 7.0). The fluorescence emission spectra of the albumins exhibited in the presence of the compounds a significant quenching of the SA fluorescence emission band at $\lambda_{em,max}$ = 343 nm with the simultaneously appearance of a second emission band at 409 nm.

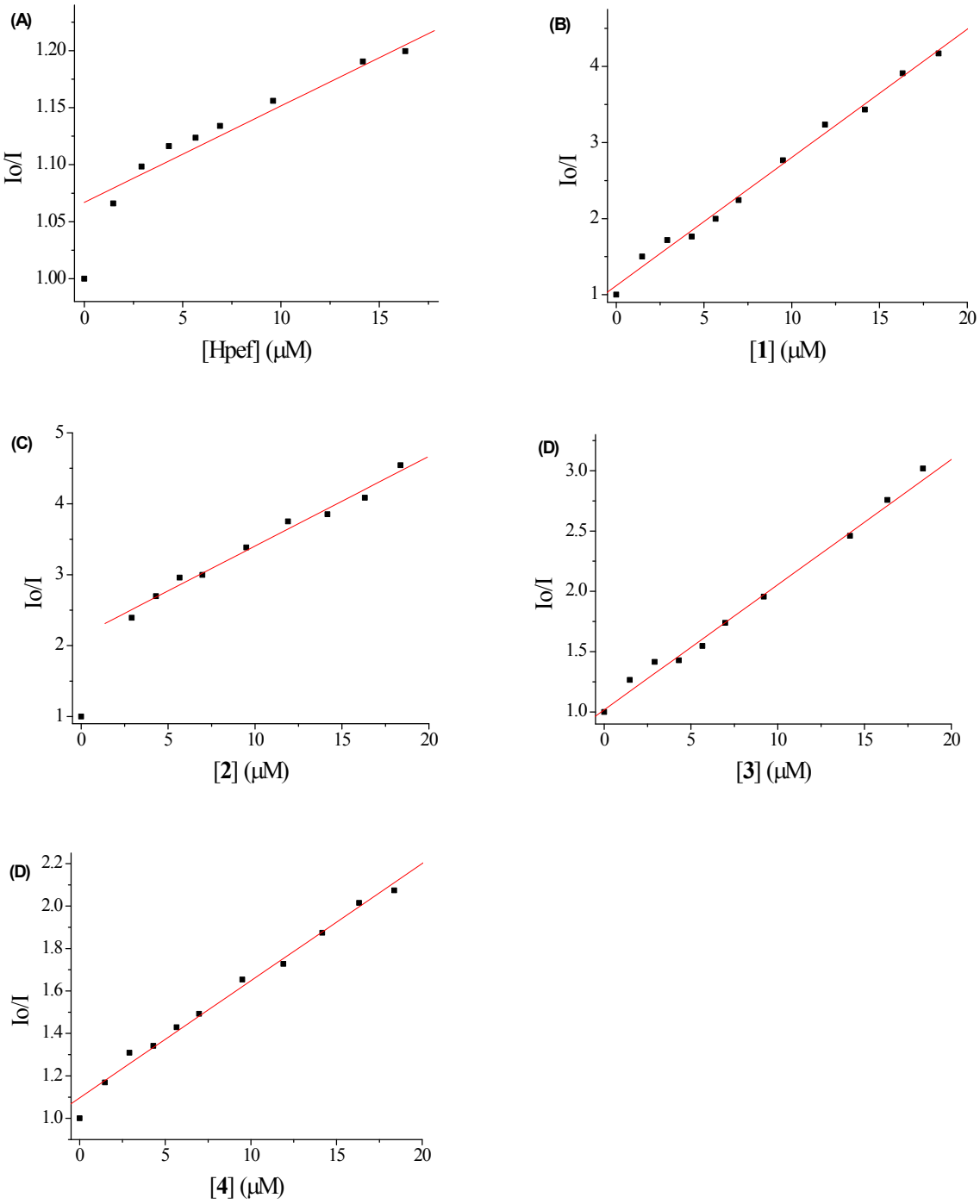

Figure S4. Stern-Volmer quenching plot of BSA (A) Hpef and (B)-(E) complexes **1**-**4**, respectively.

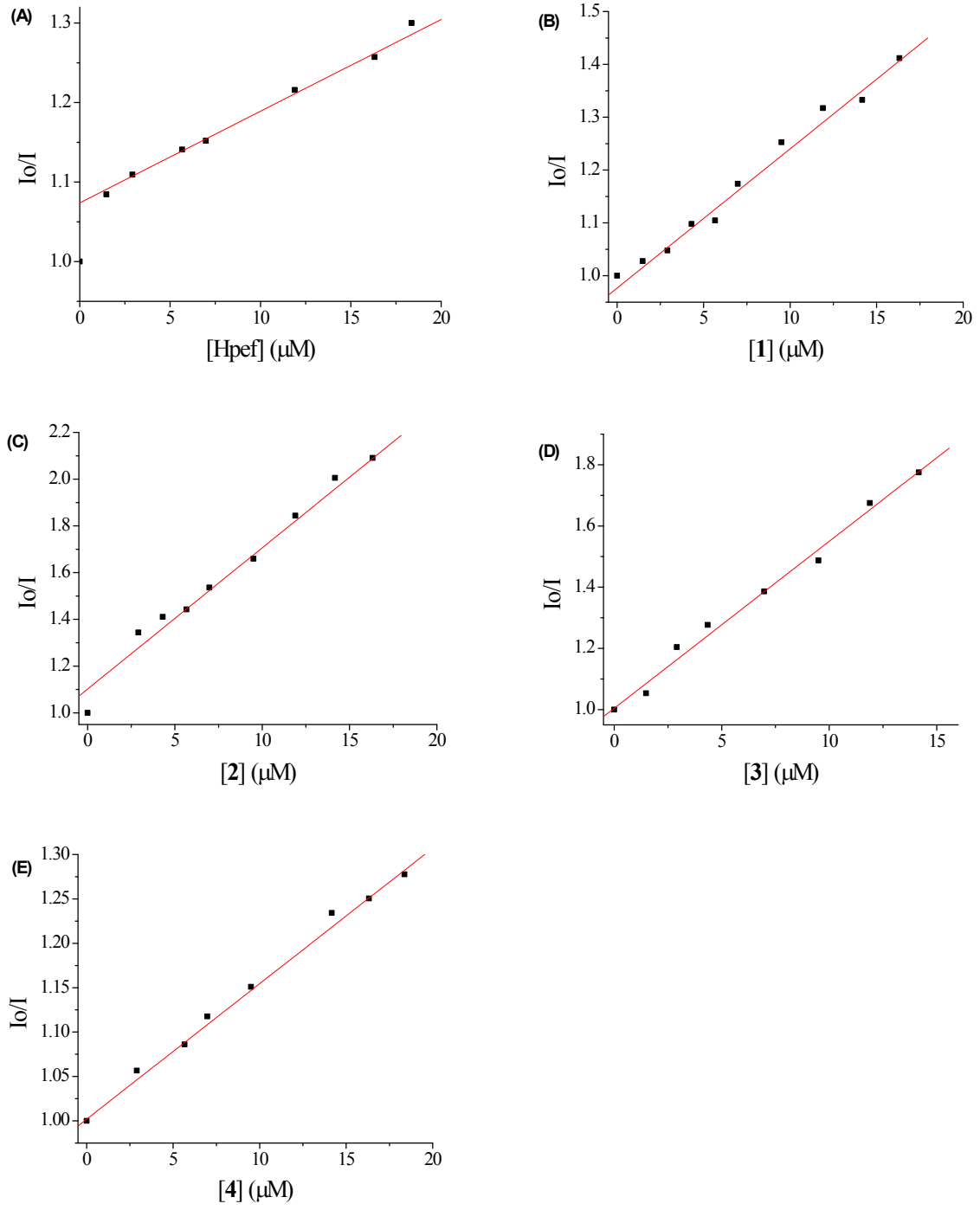

Figure S5. Stern-Volmer quenching plot of HSA (A) Hpef and (B)-(E) complexes **1**-**4**, respectively.

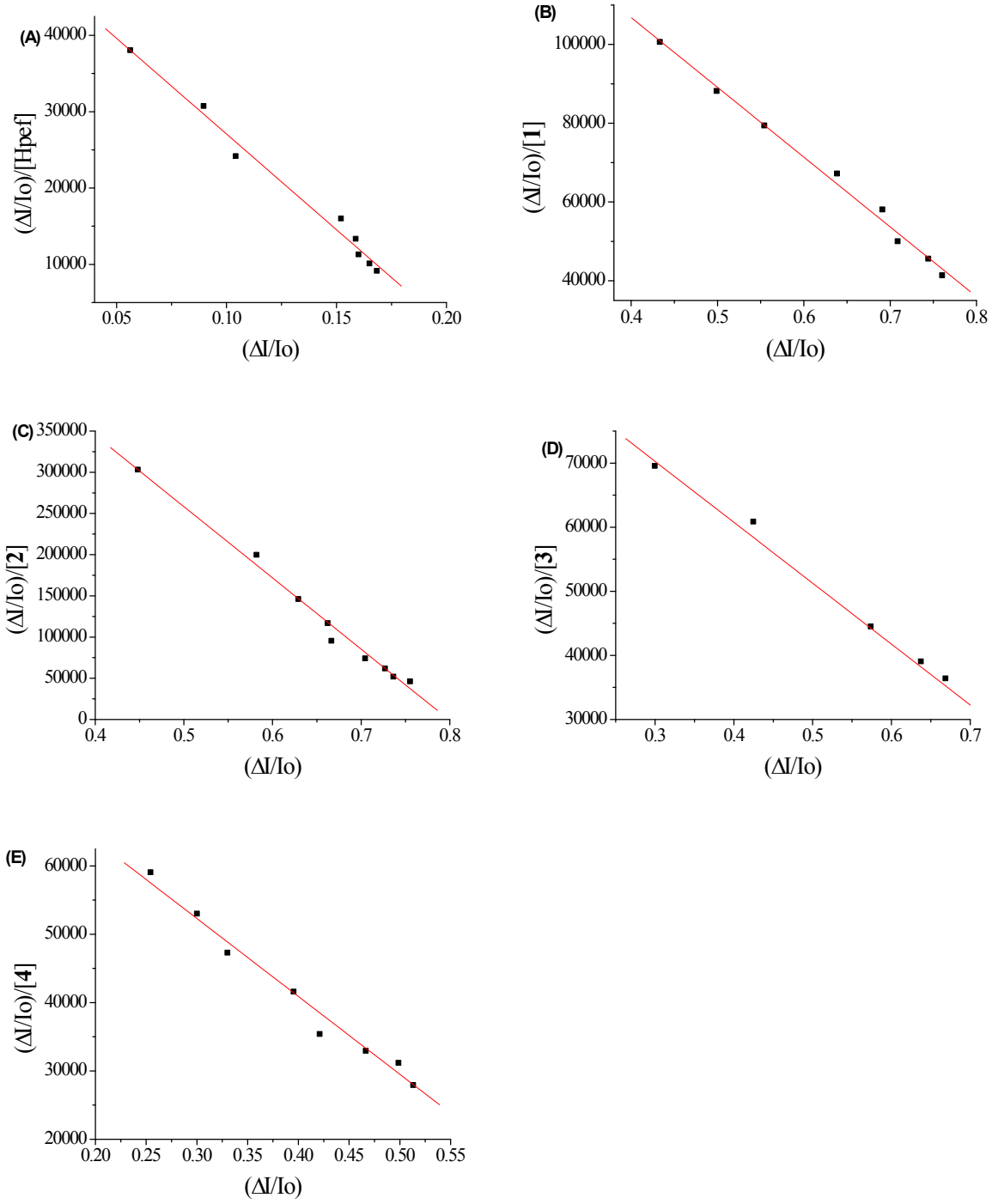

Figure S6. Scatchard plot of BSA for (A) Hpef and (B)-(E) complexes **1**-**4**, respectively.

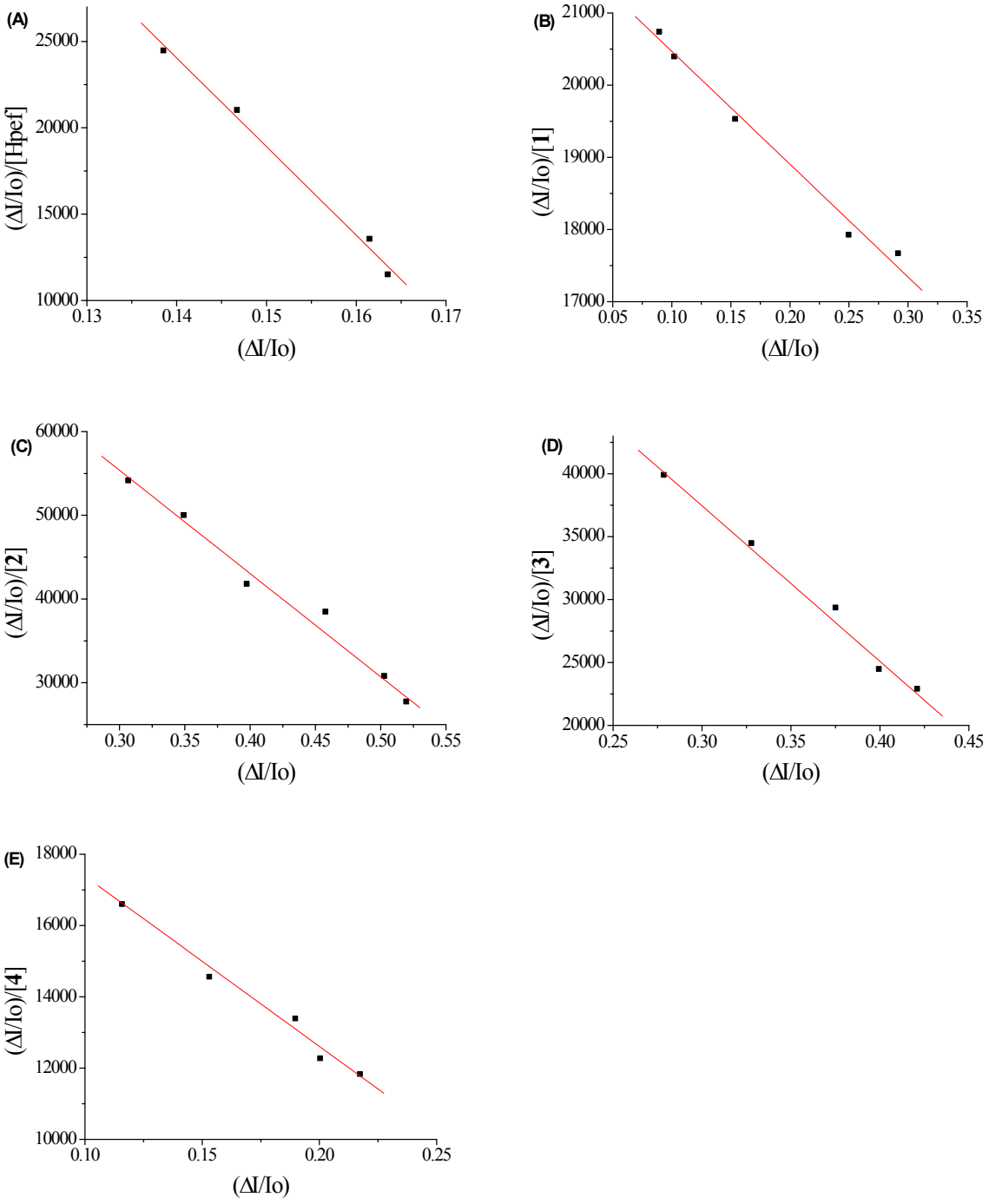

Figure S7. Scatchard plot of HSA for (A) Hpef and (B)-(E) complexes **1**-**4**, respectively.

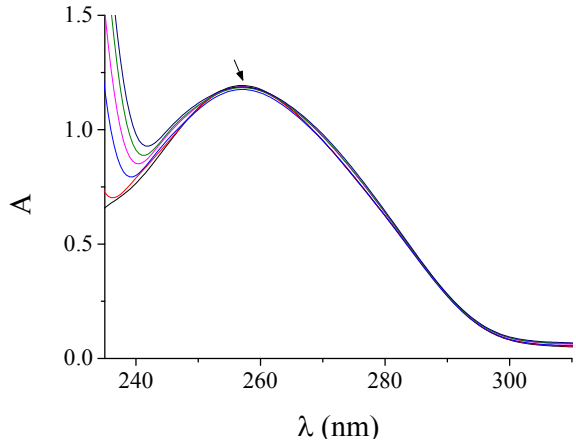

Figure S8. UV-vis spectra of a buffer solution (15 mM trisodium citrate and 150 mM NaCl at pH 7.0) of CT DNA (1.80×10^{-4} M) in the presence of increasing amounts of complex **1**. The arrow shows the changes upon increasing amounts of the complex. The DNA-band at λ_{max} = 258 nm exhibits in the presence of the compounds at increasing amounts a slight hypochromism accompanied by a red-shift up to 261 nm. Similar changes have been observed in the UV-vis spectra of CT DNA in the presence of increasing amounts of complexes **2-4.** These changes may indicate the interaction of the compounds with CT DNA which may lead to a new complex-DNA conjugate.

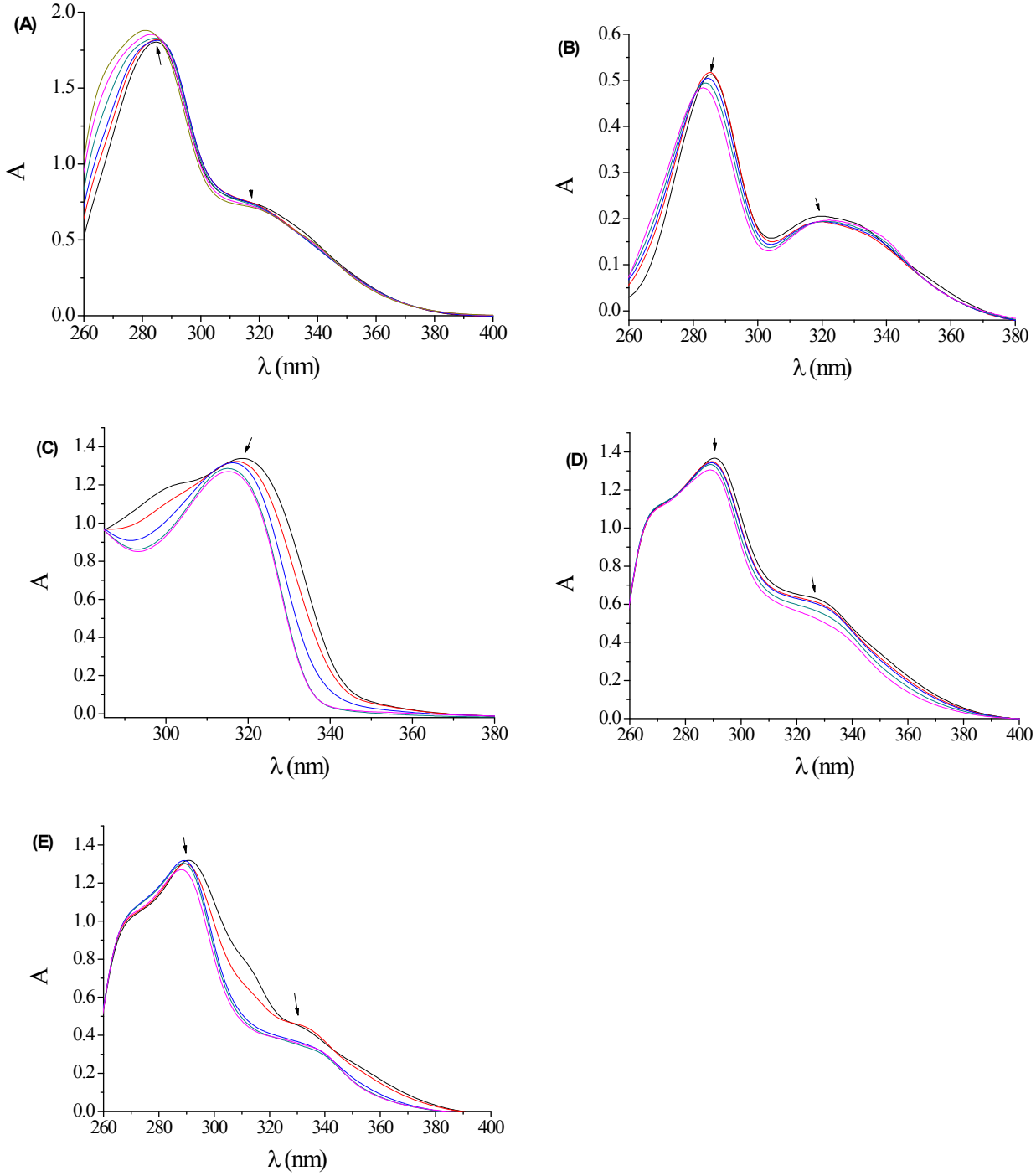

Figure S9. UV-vis spectra of DMSO solution of complex (A) Hpef ([Hpef] = 10 μM), (B) **1** ([**1**] = 10 μM), (C) **2** ([**2**] = 20 μM), (D) complex **3** ([**3**] = 20 μM) and (E) **4** ([**4**] = 10 μM) in the presence of increasing amounts of CT DNA (r' = 0-1.0). The arrows show the changes upon increasing amounts of CT DNA. The intraligand bands exhibited in the presence of increasing amounts of CT DNA a hypochromism which was much more pronounced (up to 30%) for complexes **3** and **4.** The observed hypochromism in the UV-vis spectra of the compounds may be attributed to π→π stacking interaction between the aromatic chromophores (from the quinolone and/or the N,N´-donor ligands) of the complexes and DNA-bases.

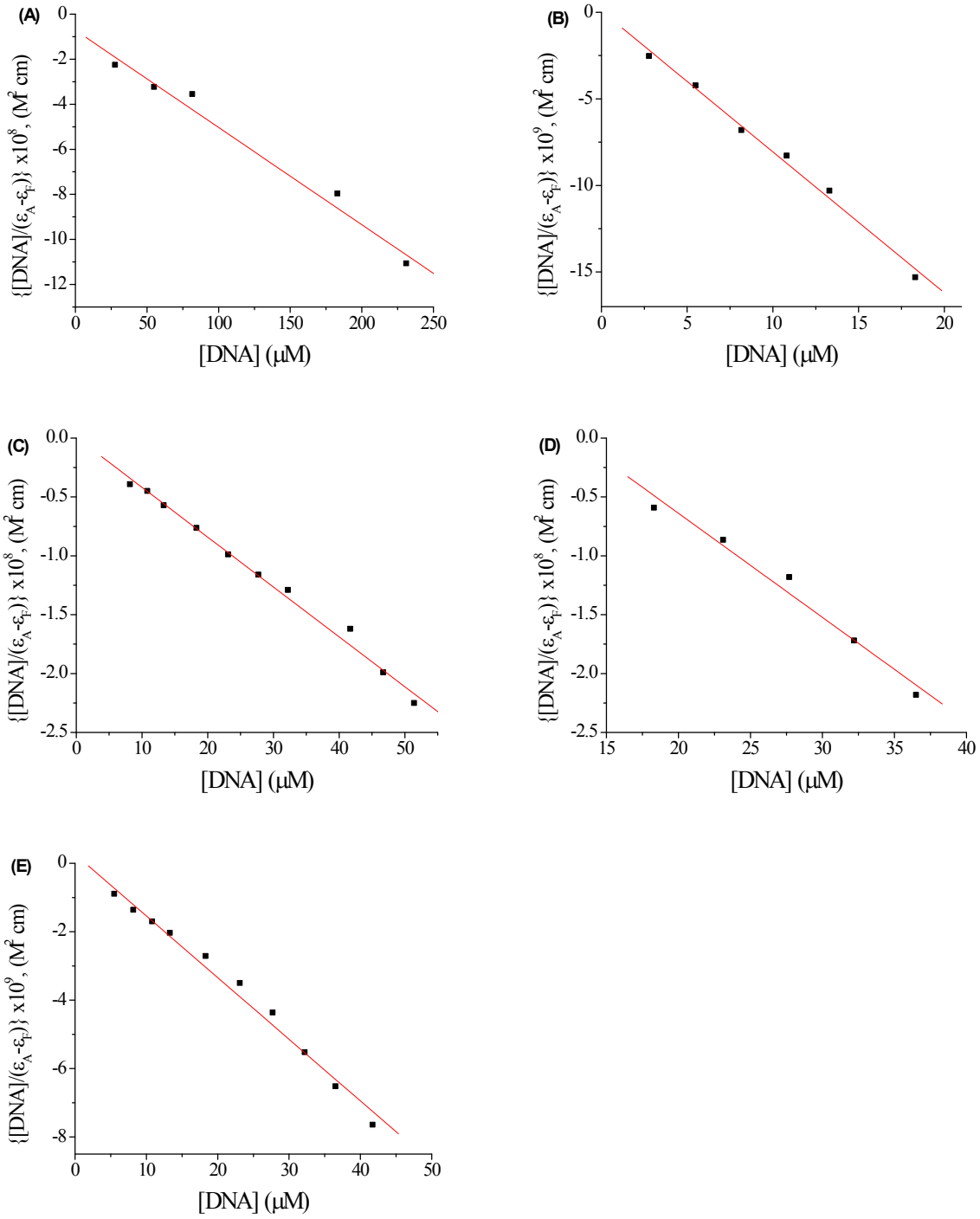

Figure S10. Plot of [DNA]/(ε_A-ε_f) *versus* [DNA] for (A) Hpef and (B)-(E) complexes **1**-**4**, respectively.

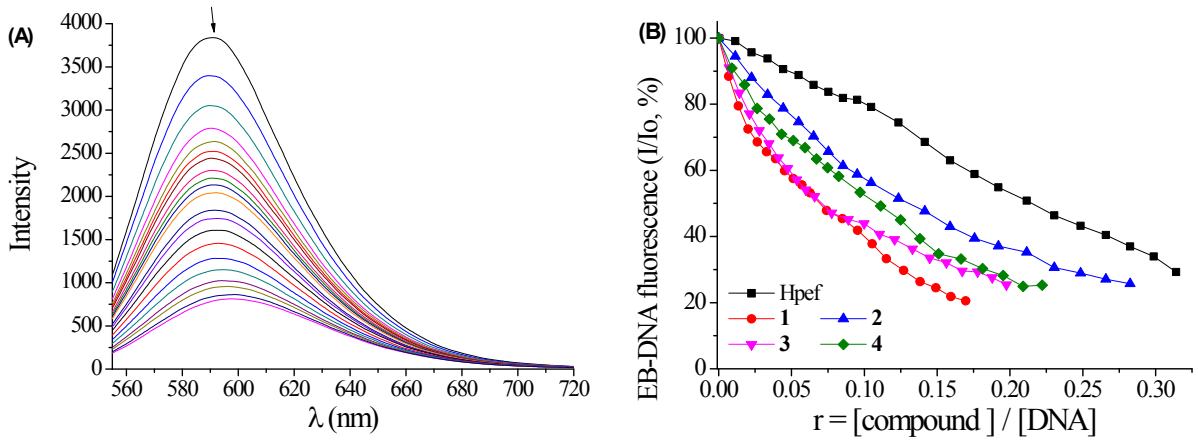

Figure S11. (A) Emission spectra (λ_{exit} =540 nm) for EB-DNA conjugate ([EB] = 20 μM, [DNA] = 26 μM) in buffer solution (150 mM NaCl and 15 mM trisodium citrate at pH = 7.0) in the absence and presence of increasing amounts of complex **1**. The arrow shows the changes of intensity upon increasing amounts of **1**. (B) Plot of EB-DNA relative fluorescence intensity at λ_{em} = 592 nm (I/Io, %) *versus* r (r = [compound]/[DNA]) in the presence of Hpef and complexes **1-4** (quenching up to 29.2% of the initial EB-DNA fluorescence for Hpef, 20.5% for **1**, 25.7% for **2,** 25.4% for **3** and 25.3% for **4**).

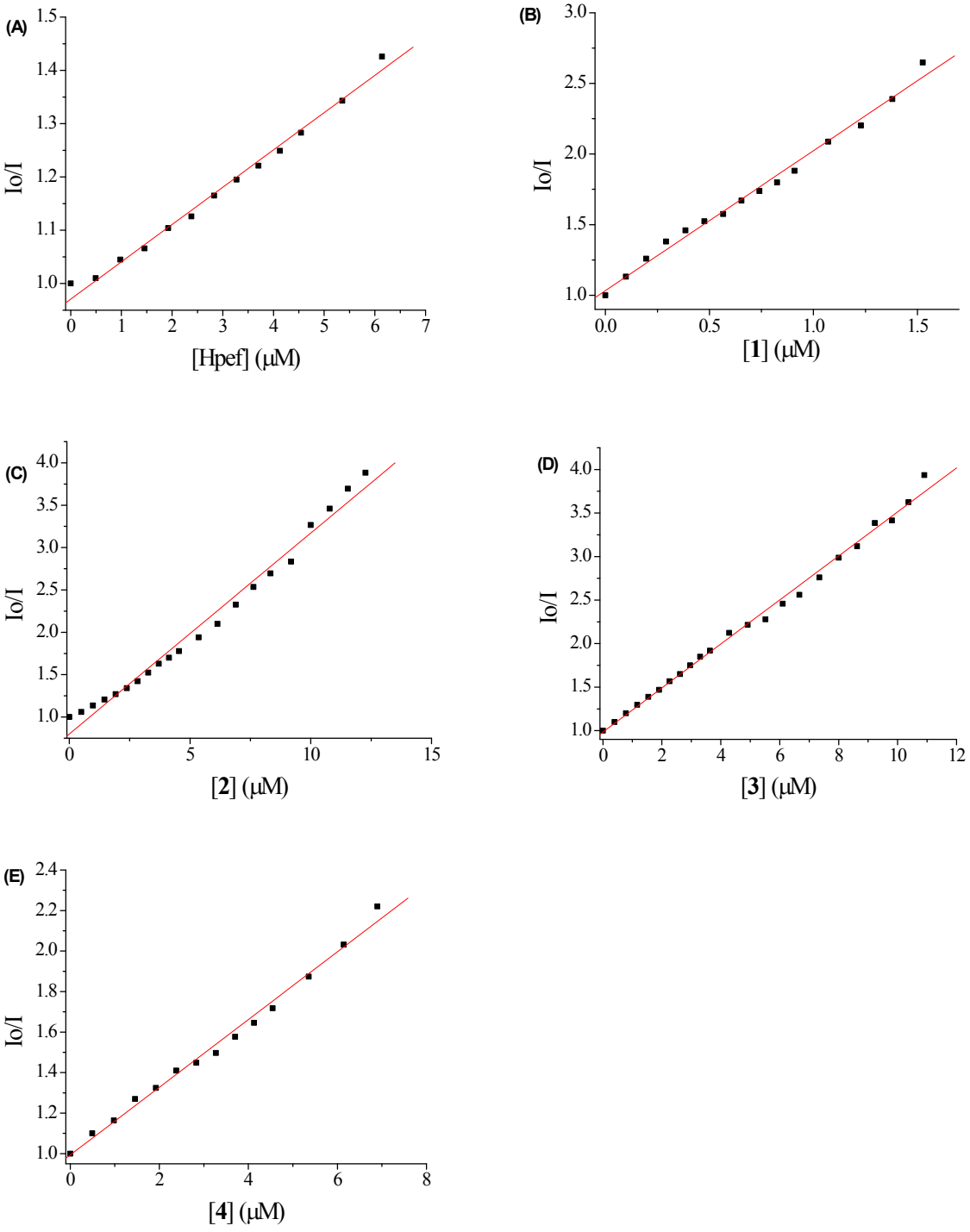

Figure S12. Stern-Volmer quenching plot of EB-DNA fluorescence for (A) Hpef and (B)-(E) complexes **1**-**4**, respectively.